



Received: 19/03/2025

Revised: 27/08/2025

Accepted: 25/09/2025

Published online: 30/09/2025

Research Article



Open Access under the CC BY -NC-ND 4.0 license

UDC 535.8

## DEVELOPMENT AND OPTIMIZATION OF OPTICAL PAYLOAD FOR NANOSATELLITES WITH STRICT CONSTRAINTS

Zhumazhanov B.R.<sup>1</sup>, Zhetpisbayeva A.<sup>2\*</sup>, Kulakayeva A.<sup>3</sup>, Makhanov K.<sup>2</sup>, Zhumazhanov B.S.<sup>1</sup><sup>1</sup> «Ghalam» LLP, Astana, Kazakhstan<sup>2</sup> L.N. Gumilyov Eurasian national university, Astana, Kazakhstan<sup>3</sup> International Information Technology University, Almaty, Kazakhstan

\*Corresponding author: aigulji@mail.ru

**Abstract.** This article presents the design and optimization of a compact, high-performance optical payload for Earth observation nanosatellites. The payload is based on a Ritchey-Chrétien telescope with corrective lenses, providing a ground sample distance (GSD) of 6 meters per pixel from a 600 km orbit while meeting strict constraints on mass, dimensions, power consumption, and operational conditions in the space environment. The design process, conducted using Zemax 2024 software, focuses on achieving high image quality within the limitations typical for a 12U CubeSat. The results confirm the feasibility of the project, ensuring a modulation transfer function value exceeding 0.26 at the Nyquist frequency. Several key performance indicators were evaluated, including the system modulation transfer function. Once the required parameters were achieved, a lens corrector system was added and the field angles were optimized. BK7 and Fused Silica were selected as lens materials. The simulation results confirm that the developed optical payload meets the requirements for use in space conditions, including resistance to vibration loads during launch vehicle launch.

**Keywords:** Earth remote sensing, modulation transfer function, payload, nanosatellite, spacecraft.

### 1. Introduction

The growing demand for Earth remote sensing (ERS) data is driving the development of nanosatellites. Miniaturization requires the creation of compact and efficient optical payloads capable of delivering high-quality images while operating under strict constraints on mass, size, and power consumption. This article presents the design and optimization of such a payload for a CubeSat 12U, aimed at achieving high spatial resolution (6 m GSD) while meeting the stringent requirements typical of the nanosatellite environment.

12U CubeSats, typically ranging in mass from 10 to 24 kg, face significant resource limitations. Power generation within these platforms generally ranges within 20-60 Watts, thereby restricting payload capabilities. In contrast, larger small satellites offer substantially greater power budgets, typically ranging from 150 Watts, and can reach up to 2000 Watts. This disparity underscores the critical need for efficient power management and optimized performance in CubeSat payload designs.

Over the past decade, there has been a significant increase in the number of remote sensing satellites launched by various governments and commercial organizations. This trend reflects the growing demand for and importance of remote sensing technologies applied in fields such as cartography, agriculture, early warning systems, and natural resource monitoring [1].

As an integral part of information technology, ERS plays a key role in providing high-precision and reliable information products essential for industry, science, and society in the modern information economy. To meet the demand for high-quality ERS data, it is critical to develop a fully functional and advanced calibration system, including measurement instruments, measurement methodologies, and a dedicated test site [2]. Manufacturers of space systems apply various standards and methods to evaluate the performance of Earth observation (EO) satellite systems. A wide range of metrics is commonly used, with the most well-known being the modulation transfer function (MTF) [3], absolute signal-to-noise ratio (SNR) [4], and geometric resolution [5]. Additional approaches include differential SNR [6], frequency-dependent SNR [6], noise-equivalent change in reflectance ( $NE\Delta\rho$ ) [7], and national image interpretability rating scales (NIIRS) for image quality assessment [2].

Thus, for a precise and comprehensive system analysis, it is necessary to integrate multiple evaluation metrics. Modern trends in the space industry, such as satellite miniaturization and the development of constellation missions, impose new requirements on optical systems. Compact and high-performance solutions are needed to ensure high-quality imaging while operating under strict mass and size constraints. The development of optical payloads for nanosatellites, such as CubeSats, presents numerous complex engineering challenges. Existing remote sensing systems provide invaluable information essential for scientific research and practical Earth-related applications [8]. In particular, multispectral images obtained from satellite systems play a key role in monitoring climate change and environmental conditions, representing the most common type of data collected by ERS satellite payloads [9].

The modern satellite systems market is characterized by a shift toward flexible and reconfigurable solutions, made possible by technological innovations such as embedded processors, active antennas, and photonic components. Satellite manufacturers are actively developing and exploring various payload configurations, striving to maximize flexibility through the use of embedded systems. This has led to an increasing number of possible configurations, requiring careful selection during satellite system design. The traditional approach to evaluating satellite system performance, based on predefined coverage characteristics and payload configurations, demands significant resources for implementation and testing. While this approach ensures high accuracy, it limits design flexibility by requiring the preselection of a limited number of configurations. This study proposes a software optimization tool that enables rapid parametric assessment of system throughput, considering different payload architectures [10].

High image quality is a critical requirement for high-precision remote sensing applications. Traditional design methods often rely on the experience of developers, which does not guarantee an optimal trade-off and may lead to suboptimal solutions [11]. In the work of Abolghasemi and Abbasi-Moghadam [12], an analysis and design methodology for an experimental remote sensing payload is presented, along with system performance results, including signal-to-noise ratio (SNR) and pre-MTF at a spatial resolution of 50 m in three spectral bands (green, red, and near-infrared). The obtained results demonstrate high image quality, with SNR > 100 and MTF > 40 for a push-broom scanner at an altitude of 700 km.

The study also describes a systematic approach to the development and performance evaluation of a multispectral payload, including an analysis of noise components such as photon noise, background noise, cold shield noise, and electronic noise. System performance was assessed using cascaded MTF, taking into account the effects of optics, image discretization, and satellite motion. The calculation results are provided for the SINA-1 satellite.

In study [13] presents the design of an optical telescope for CubeSats. The authors showed that reflector-based configurations can provide high image quality even within the strict size constraints of the platform. However, their analysis focused solely on the optical design and did not take into account thermo-mechanical stability or straylight, which limits the practical applicability of the results.

Similar limitations can be observed in the MeznSat project [14], where a SWIR spectrometer payload was implemented on a 3U CubeSat. Although the system demonstrated effectiveness for atmospheric monitoring, the study did not consider the combined impact of thermal and mechanical factors that determine image stability.

The importance of testing is highlighted in [15], which describes a thermal vacuum campaign on a CubeSat engineering model. Such experiments are valuable for identifying structural weaknesses, but the results were not directly linked to specific optical designs. This leaves open the question of how test data can be systematically integrated into the development of optical payloads.

A more detailed exploration of CubeSat optical instrumentation is presented in the KITSUNE mission [16]. A focusing mechanism was implemented that achieved image quality with a ground sampling distance

of several meters. At the same time, the issue of long-term focusing stability under thermal variations and vibrations remained unresolved, which limits the practical applicability of the results for Earth observation tasks. A similar conclusion can be drawn from the HiREV project [17], where a camera with a resolution of up to 3 m was demonstrated. This confirmed the potential of CubeSats for high-resolution Earth observation, but the study concentrated on imaging performance while leaving aside issues of straylight suppression and thermo-mechanical optimization.

Thermo-mechanical aspects were addressed in more depth in [18], where mechanical and thermal analyses of a 12U CubeSat carrying a LIDAR payload were conducted. Nevertheless, the authors did not assess how the identified deformations affected image quality, again underscoring the fragmented nature of existing approaches. Another line of research involves the use of phase change materials (PCM) for thermal stabilization. In [19], it was shown that PCM can smooth temperature peaks and improve the stability of multispectral payload performance. However, incorporating such solutions into small satellites remains difficult due to strict mass and volume constraints, as well as the lack of methodologies linking thermal control to optical performance.

Overall, the literature shows that research on CubeSat optical payloads is active and covers a wide spectrum of topics – from telescope and spectrometer design to testing campaigns and thermal stabilization methods. Yet, these efforts remain fragmented: optical systems are often analyzed without considering thermal effects, testing is performed without connection to specific designs, or stabilization methods are proposed without addressing straylight suppression. This indicates that the comprehensive problem of ensuring thermo-mechanical stability and minimizing straylight under the strict mass, size, and power constraints of CubeSats remains unresolved.

## 2. Materials and methods. Optical system design

The telescope was designed using Zemax 2024 based on the Ritchey-Chrétien configuration. This design was chosen for its effectiveness in minimizing spherical aberration and coma, which are critical for achieving high-quality imaging within the system's compact constraints. To meet the required spatial resolution of 6 m at an orbital altitude of 600 km, the optical system was developed with two hyperbolic mirrors and a corrective lens system. The lens materials selected were BK7 and fused silica. BK7 offers high transparency in the visible spectrum. Fused silica exhibits similar transparency but also features a wider spectral range, making it suitable for applications requiring broader wavelength coverage.

The Ritchey-Chrétien telescope design aims to achieve maximum resolving power while maintaining optimal mass and dimensional characteristics. This system represents a modified Cassegrain configuration, featuring hyperbolic primary and secondary mirrors, which effectively minimize spherical aberrations and coma, ensuring a wide field of view with high accuracy. A corrective lens system has been integrated to compensate for field curvature, which arises when using a flat detector.

As the imaging detector, we employed the CMV12000 CMOS sensor (ams/CMOSIS). The device provides a resolution of  $4096 \times 3072$  pixels ( $\approx 12.5$  MP) with a  $5.5 \mu\text{m}$  pixel pitch, corresponding to an active area of  $22.5 \times 16.9$  mm (diagonal  $\approx 28.1$  mm). The architecture is based on a global shutter with an 8T pixel design and correlated double sampling, which reduces fixed-pattern noise and enables exposure during readout. The sensor supports 8/10/12-bit quantization and features 64 LVDS outputs at up to 600 Mbit/s per channel, enabling frame rates of up to  $\approx 132$  fps at full resolution (12 bit) and  $\approx 300$  fps in windowed readout modes.

The typical peak quantum efficiency of the monochrome version is 50–60% around 550 nm, enhanced further by microlenses that improve the effective fill factor. Key sensitivity parameters include temporal noise of about  $13 \text{ e}^- \text{ rms}$ , dark current of approximately  $70 \text{ e}^-/\text{s}$  at  $25^\circ\text{C}$ , a maximum SNR of  $\approx 41$  dB, and a dynamic range of  $\approx 60$  dB. The CMV12000 is an area-scan sensor without native TDI functionality; its use in push broom configurations is only possible with external scanning and does not provide charge accumulation along detector rows.

It is important to note that using classical manufacturing methods for such telescopes with relatively large apertures would lead to an increase in satellite mass and volume. However, several innovative techniques can reduce telescope size [20]. For example, the synthetic aperture concept allows for the segmentation of a monolithic primary mirror into smaller foldable segments, which are deployed after the satellite reaches orbit [21]. Another emerging technology, based on adaptive optics, enables the realization of a 1.5-meter mirror

[22]. Recently, a 1.3-meter large-aperture mirror was developed using lightweight space optical components [23].

### 3. Results

Calculation of key parameters:

The focal length of the telescope plays an important role in determining the quality and characteristics of the obtained images. The focal length ( $f$ ) of the telescope is calculated using the formula:

$$f = \frac{H\Delta}{GSD}; \quad (1)$$

where  $H$  is the orbit height (600 km),  $\Delta$  is the detector pixel size (5.5  $\mu\text{m}$ ), and GSD is the required ground sample distance (6 m). The calculation gives a focal length of approximately  $f \approx 550$  mm.

The minimum aperture diameter ( $D$ ) of the telescope is determined by the formula:

$$D \geq \frac{1,22 * \lambda * f}{\Delta}; \quad (2)$$

where  $\lambda$  is the minimum wavelength (450 nm for RGB). The calculation gives a minimum aperture diameter of approximately 54.9 mm. Considering dimensional constraints (the aperture diameter must fit within 1U of a CubeSat) and the need to accommodate additional components, the aperture diameter was set to 85 mm.

The field of view (FoV) of the telescope is calculated using the formula:

$$FoV = 2 \arctan \frac{SW}{2H}; \quad (3)$$

where  $SW$  is the swath width (30,720 m, calculated based on the detector resolution and GSD). The calculation gives  $FoV \approx 3^\circ$ .

The telescope's f-number ( $f\#$ ) is calculated as:

$$f\# = F/D = 6,47 \quad (4)$$

Based on the obtained parameters, the optical system was designed and simulated, with its schematic shown in Figure 1. The modulation transfer functions (MTF) graph for this system is presented in Figure 2.

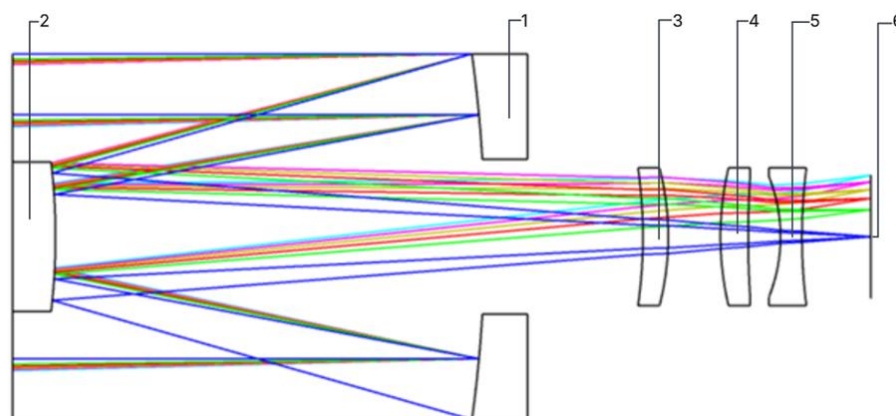


**Fig.1.** Optical diagram of the developed payload:

1 – primary mirror, 2 – secondary mirror, 3 – first lens corrector, 4 – second lens corrector, 5 – third lens corrector, 6 – detector plane.

The MTF is a key metric for assessing image quality in optoelectronic imaging systems. MTF is defined as the spatial frequency response of the system, representing its ability to reproduce sinusoidal test patterns of varying spatial frequencies. The overall image quality of the system—system MTF—is determined by the contributions of each of its components, as each element plays a role in shaping the final image.

Image quality is significantly affected by the optical system, the detector, blurring effects, and atmospheric conditions. According to the technical requirements, the MTF value of the designed telescope must exceed 0.1 at the Nyquist frequency (91 line pairs/mm). Simulation results have shown that the developed telescope achieves an optical system MTF value of 0.26 at the Nyquist frequency (Fig. 2).

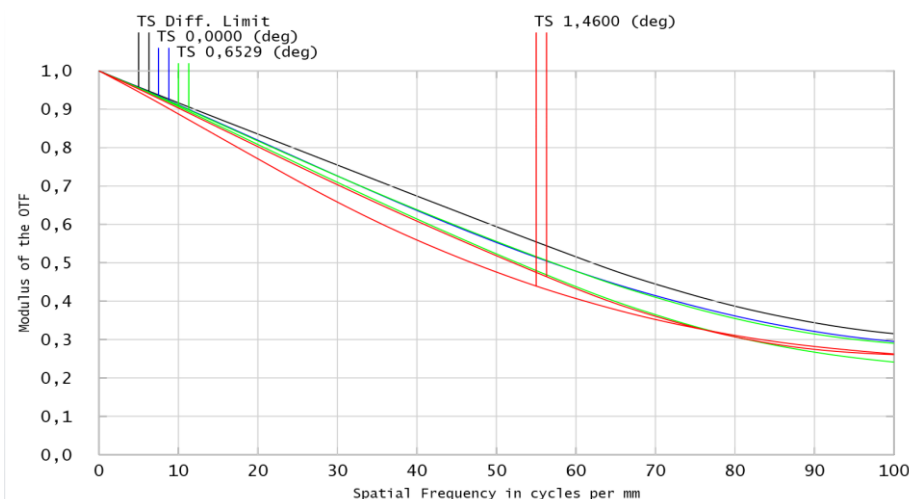


**Fig.2.** Modulation transfer function graph for the developed payload

The mirror segment of the system was designed and optimized independently of the corrective lens system, with calculations performed solely along the optical axis. This approach minimized the impact of lens defocusing on image quality. Once the required characteristics of the mirror system were achieved, corrective lenses were integrated, and additional optimization of the field angles was carried out.

BK7 and fused silica were selected as the lens materials.

BK7 provides high transparency in the visible spectral range.

Fused silica offers high transparency over a broader spectral range and exhibits enhanced radiation resistance.

Two materials were selected for the fabrication of corrective lenses: optical glass BK7 and fused silica. The choice was based on their optical and mechanical properties. BK7 is characterized by a high refractive index ( $n_d = 1.5168$ ) and moderate dispersion ( $v_d = 64.17$ ), providing sufficient transparency in the visible range (330–2100 nm). Fused silica exhibits a lower refractive index ( $n_d = 1.4585$ ) and even lower dispersion ( $v_d = 67.82$ ), while offering a significantly broader transmission range (180–3500 nm) and high thermal stability (thermal expansion coefficient of  $0.55 \times 10^{-6}/^{\circ}\text{C}$ ).

Additionally, fused silica has high chemical resistance and is highly resistant to UV radiation and laser exposure. Thus, the selection of these materials ensures an optimal combination of optical performance and durability for operation in space conditions.

The Point Spread Function (PSF) is one of the most important characteristics of an optical system, describing the distribution of light intensity in the image of a point source. PSF analysis allows for the assessment of image quality, which is determined by factors such as resolution, contrast, and the presence of aberrations. The graphical representation of the PSF is a scatter diagram that illustrates the distribution of light intensity in the focal plane depending on the position on the detector.

The shape and size of the scatter spot are directly related to the presence and magnitude of aberrations in the optical system, as well as diffraction effects. A compact and symmetrical scatter spot indicates high image quality, whereas a blurred or asymmetrical spot suggests the presence of aberrations and a decrease in image quality. Analyzing the PSF at various distances from the optical axis (across the field of view) allows for the evaluation of the uniformity of image quality across the entire frame.

Figures 3-4 present the PSF for the developed optical system, obtained through Zemax simulations. Figure 3 illustrates the PSF of the telescope without the corrective lens system, while Figure 4 shows the PSF with the corrective lens system integrated.

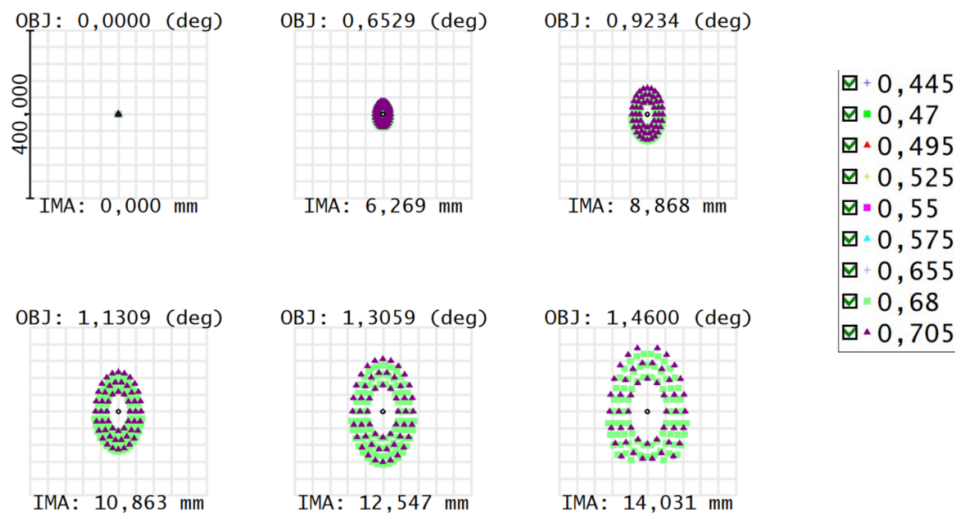


**Fig.3.** Ray spot diagram for telescope without a corrective lens system

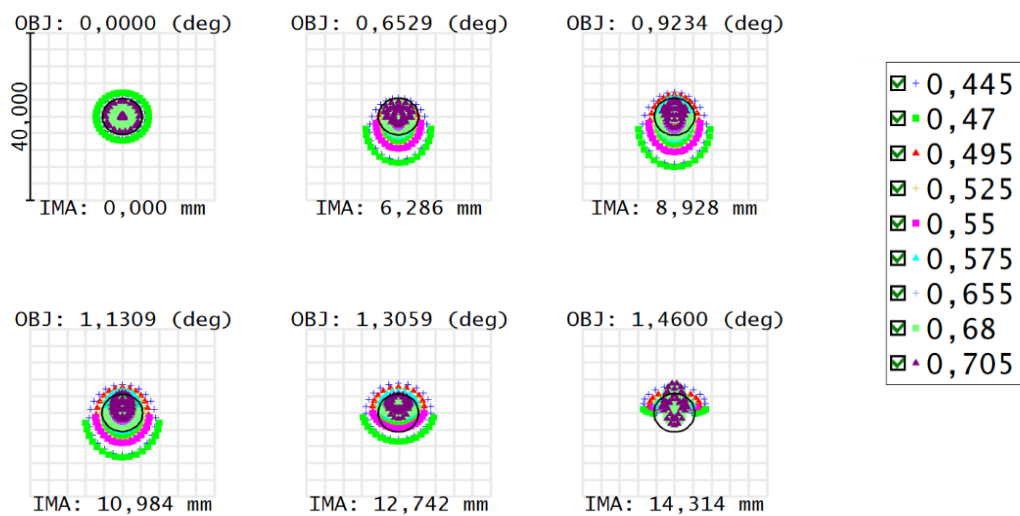


**Fig.4.** Ray spot diagram for telescope with a corrective lens system

Simulation results show that in the absence of corrective lenses (Fig. 3), the telescope forms an almost perfect image at the center of the field of view; however, a significant increase in spot size and distortion of its shape is observed toward the edges. The inclusion of a corrective lens system (Fig. 4) leads to a slight degradation of image quality at the center, characterized by a small increase in spot size. However, this degradation is minimal compared to the significant improvement in image quality at the periphery of the field of view, where a substantial reduction in spot size and a more symmetrical shape are observed. This confirms the effectiveness of the corrective lens system in minimizing aberrations and enhancing image quality across the entire field of view. The Table 1 summarizes the parameters of the optical payload.

To mitigate direct illumination of the detector via the front aperture of the system and the central aperture of the primary mirror, the straylight analysis was done, and by its results, the external and internal baffles were designed and implemented. The effectiveness of these elements was assessed using non-sequential ray tracing simulations within Zemax OpticStudio. The configuration of the baffles is illustrated in Figure 5.



While not providing complete shielding of direct flight paths, this baffle contributes to reducing the intensity of scattered light originating from external sources outside the primary field of view, thereby minimizing background stray light, particularly crucial in high-illumination environments.

**Table 1.** Parameters of optical payload.

#	Payload parameters	Values
1	Reference Orbit type	Sun Synchronous
2	Reference Orbit Altitude	600 km
3	Size	3U
4	Mass	<2,0 kg
5	Image size (from reference orbit)	18 km x 24 km
6	GSD (from reference orbit)	6 m
7	Onboard memory	128 GB
8	MTF	> 0.26
9	Life time	2 years

As an additional way of reduction of straylight, the Acktar foil was applied to the internal surfaces of the tube. Coating internal parts of the tube by Acktar foil allows to absorb an exceptionally high percentage of incident light. This greatly reduces the amount of light that can be reflected or scattered within the optical system.

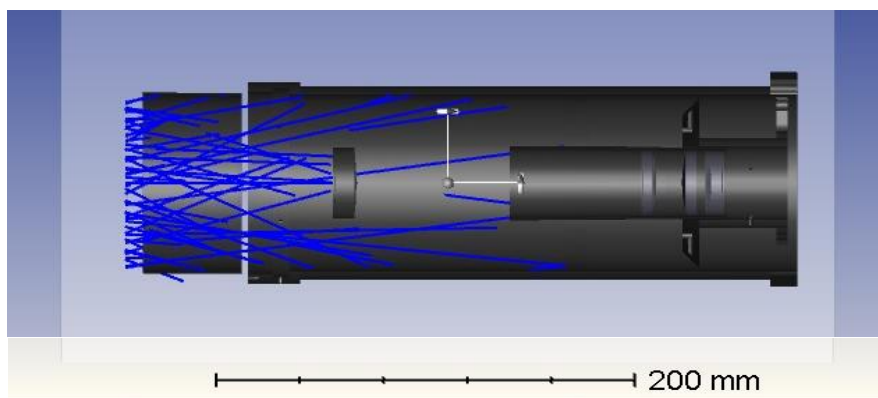


**Fig. 5.** Model of baffle placement within the optical system)

#### 4. Discussion

The optimized optical system achieved the target GSD of 6 meters at an orbital altitude of 600 km. MTF analysis showed an exceeding of the target value, with an MTF of 0.26 at the Nyquist frequency. Scatter diagrams confirmed high image quality across the entire field of view. Detailed modeling assessed the structural stability under various space environment factors.

The presented work demonstrates the feasibility of developing a high-performance optical payload for nanosatellites capable of capturing high-quality images of Earth. The Ritchey-Chrétien design effectively balances high performance with constraints on mass, dimensions, and power consumption. Further research may focus on the application of advanced methods in the development of solutions for the payload electronics module. The Ritchey-Chrétien design was selected as it provides superior off-axis performance at compact size of the payload. This design corrects for coma and astigmatism to provide a wide enough, flat field of view crucial for efficient Earth observation. While the main mission was technology demonstration, obtaining a GSD of 6 meters enables a range of applications, including the identification of individual agricultural fields, allowing for precise monitoring of crop health, as well as object recognition of objects of the corresponding size, such as automobiles and trucks. The MTF analysis revealed a performance exceeding the design goal, achieving a value of 0.26 at the Nyquist frequency. This ensures the capture of sufficiently detailed images. The article covers the current status of optical design. The work will be continued with research of methods for the straylight analysis, mechanical analysis, integration of the sensor and electronics unit to the payload and integration of the payload to satellite platform.

## 5. Conclusion

In this article, the task of designing and optimizing a compact optical payload for a CubeSat 12U spacecraft was successfully accomplished. The use of a Ritchey-Chrétien telescope with corrective lenses enabled the creation of a system that effectively minimizes spherical aberration and coma, which is crucial for ensuring high image sharpness. It was established that even with significant constraints on mass and dimensions, achieving a high spatial resolution of 6 meters at an orbital altitude of 600 km is possible.

As a result of optimizing the optical design, significant efficiency in the use of photonic components was achieved, improving system performance while maintaining its compactness. These enhancements open new prospects for the development of future nanosatellites capable of performing complex remote sensing tasks with high precision and minimal resource consumption.

Further research and development may include the design of more advanced onboard control and data processing systems for remote sensing, enhancing the overall functionality and reliability of satellite systems.

Thus, this article highlights the importance of integrating the latest technological advancements in aerospace engineering and emphasizes the significance of scientific research in space technologies, contributing to the strengthening of technological independence and the development of the national space industry.

### Conflict of interest statement

The authors declare that they have no conflict of interest in relation to this research, whether financial, personal, authorship or otherwise, that could affect the research and its results presented in this paper.

### CRedit author statement

**Zhumazhanov B.:** Project administration, Supervision, Writing - Original Draft, Methodology. **Zhetpisbayeva A.:** Investigation, Writing- Original draft, Writing- Reviewing and Editing, Conceptualization; **Makhanov K., Kulakayeva A.:** Writing- Reviewing and Editing, Investigation. **Zhumazhanov Bexultan:** Conceptualization, Methodology, Validation, Formal analysis. The final manuscript was read and approved by all authors.

### Acknowledgements

The work was carried out with financial support from the CS MES RK under the PTF program, grant BR27198365 "Development of an optoelectronic system in the short-wave infrared spectral range in the context of the development of Kazakhstan's remote sensing space systems" (2024–2026).

## References

- 1 Simon Jones, Karin Reinke (2009). *Innovations in remote sensing and photogrammetry*. Springer Science & Business Media, 468. <https://doi.org/10.1007/978-3-540-93962-7>
- 2 Li, C.R., Tang, L.L., Ma, L.L., Zhou, Y.S., Gao, C.X., Wang, N., Zhu, X. H. (2015). Comprehensive calibration and validation site for information remote sensing. *The International Archives of the Photogrammetry, Remote Sensing and Spatial Information Sciences*, XL-7/W3, 1233-1240. <https://doi.org/10.5194/isprsarchives-XL-7-W3-1233-2015>
- 3 Xing, K., Cao, S. X., Yue, C. Y., Zhou, N. (2017). Optimization design method of optical remote sensor based on imaging chain simulation. *MATEC Web of Conf.*, 114, 04013. <https://doi.org/10.1051/mateconf/201711404013>
- 4 Kramer, H. J. (2002). *Observation of the Earth and Its Environment: Survey of Missions and Sensors*, Heidelberg, Berlin, New York Berlin: Springer, 1509. <https://doi.org/10.1007/978-3-642-97678-0>
- 5 Musabayev, T. A., Moldabekov, M. M., Nurguzhin, M. R., Dyussenev, S. T., Murushkin, S. A., Albazarov, B. S., & Ten, V. V. (2013). Earth observation system of the Republic of Kazakhstan. *Proceedings of the Intern. Astronautical Congress, IAC*, 2738-2740. <https://www.eoportal.org/satellite-missions/kazeosat-2#eop-quick-facts-section>
- 6 Fiete, R. D., & Tantaló, T. (2001). Comparison of SNR image quality metrics for remote sensing systems. *Optical Engineering*, 40(4), 574-585. <https://doi.org/10.1117/1.1355251>
- 7 Citroen, M., Raz, G., & Berger, M. (2008). Noise equivalent reflectance difference (NERD) vs. spatial resolution (SR) as a good measure for system performances. *Remote Sensing System Engineering*, 7087, 66-76. <https://doi.org/10.1117/12.794632>
- 8 Attia, W. A., Eltohamy, F., & Bazan, T. M. (2020). Design of very high resolution satellite telescopes part II: comprehensive performance assessment. *IEEE Transactions on Aerospace and Electronic Systems*, 56(5), 4049-4055. <https://doi.org/10.1109/TAES.2020.2991622>
- 9 Wong, S. (2014). Predicting image quality of surveillance sensors. *Defence Research and Development Canada*, 38. Available at: [D68-2-97-2014-eng](https://www.drdc.gc.ca/D68-2-97-2014-eng)



- 10 Mengali, A., Ginesi, A., D'Addio, S. (2020). Computer-aided payload architecture optimization for HTS satellites. *Proceedings of the 10<sup>th</sup> Advanced Satellite Multimedia Systems Conference and the 16<sup>th</sup> Signal Processing for Space Communications Workshop (ASMS/SPSC)*, 1-8. <https://doi.org/10.1109/ASMS/SPSC48805.2020.9268888>
- 11 Jafarsalehi, A., Asl, E. P., & Mirshams, M. (2014). Satellite imaging payload design optimization. *Aerospace Science and Technology*, 39, 145-152. DOI:10.1016/j.ast.2014.09.003
- 12 Abolghasemi, M., & Abbasi-Moghadam, D. (2012). Design and performance evaluation of the imaging payload for a remote sensing satellite. *Optics & Laser Technology*, 44(8), 2418 - 2426. <https://doi.org/10.1016/j.optlastec.2012.04.006>
- 13 Şanlı, A., & Erkeç, T. Y. (2024). Design and Analysis of Optical Telescope Subsystem. *Journal of Aeronautics and Space Technologies*, 17(Special Issue), 92-101. URL [jast.hho.msu.edu.tr](http://jast.hho.msu.edu.tr)
- 14 Jallad, A. H., Marpu, P., Abdul Aziz, Z., Al Marar, A., & Awad, M. (2019). MeznSat—A 3U CubeSat for monitoring greenhouse gases using short wave infra-red spectrometry: Mission concept and analysis. *Aerospace*, 6(11), 118. <https://doi.org/10.3390/aerospace6110118>
- 15 Dunwoody, R., Reilly, J., Murphy, D., Doyle, M., Thompson, J., Finneran, G., ... & McBreen, S. (2022). Thermal vacuum test campaign of the EIRSAT-1 engineering qualification model. *Aerospace*, 9(2), 99. <https://doi.org/10.3390/aerospace9020099>
- 16 Jung, J., Sy, N. V., Lee, D., Joe, S., Hwang, J., & Kim, B. (2020). A single motor-driven focusing mechanism with flexure hinges for small satellite optical systems. *Applied Sciences*, 10(20), 7087. <https://doi.org/10.3390/app10207087>
- 17 Azami, M. H. B., Orger, N. C., Schulz, V. H., Oshiro, T., Alarcon, J. R. C., Maskey, A., ... & KITSUNE Team Members. (2022). Design and environmental testing of imaging payload for a 6 U CubeSat at low Earth orbit: KITSUNE mission. *Frontiers in Space Technologies*, 3, 1000219. <https://doi.org/10.3389/frspt.2022.1000219>
- 18 Guentchev, G. N., Bayer, M. M., Li, X., & Boyraz, O. (2021, August). Mechanical design and thermal analysis of a 12U CubeSat MTCW lidar based optical measurement system for littoral ocean dynamics. *CubeSats and SmallSats for Remote Sensing V*, Vol. 11832, 71-98. <https://doi.org/10.1117/12.2597709>
- 19 Geismayra, L., Schumma, F., Langer, M., Binder, M., & Schlick, G. (2020, October). Thermo-Mechanical Design and Analysis of a Multispectral Imaging Payload using Phase Change Material. *Proceeding of the Intern. Astronautical Congress (IAC) – The CyberSpace Edition*, 1-17, IAC-20-C2.5.13 <https://www.researchgate.net/publication/348603407>
- 20 Woodruff, R. A., Hull, T., Heap, S. R., Danchi, W., Kendrick, S. E., & Purves, L. (2017). Optical design for CETUS: a wide-field 1.5 m aperture UV payload being studied for a NASA probe class mission study. *Astronomical Optics: Design, Manufacture, and Test of Space and Ground Systems*, 10401, 400 - 408. <https://doi.org/10.48550/arXiv.1912.06763>
- Contreras, J. W., & Lightsey, P. A. (2004, October). Optical design and analysis of the James Webb Space Telescope: optical telescope element. *Novel Optical Systems Design and Optimization VII* 5524, 30 - 41. <https://doi.org/10.1117/12.559871>
- 21 Devilliers, C., Du Jeu, C., Costes, V., Suau, A., Girault, N., & Cornillon, L. (2017). New design and new challenge for space large ultralightweight and stable Zerodur mirror for future high resolution observation instruments. *Proceedings of the Intern. Conf. on Space Optics—ICSO 2014*, 10563, 442-450. <https://doi.org/10.1117/12.2304187>
- 22 Wang, X., Guo, C., Liu, Y., Chen, J., Wang, Y., & Hu, Y. (2019). Design and manufacture of 1.3 meter large caliber light-weighted Space optical components. *Proceedings of the Intern. Conf. on Space Optics—ICSO 2018*, 11180, 304-321. <https://doi.org/10.1117/12.2535947>

## AUTHORS' INFORMATION

**Zhumazhanov, Berik** – Master (Sci.), Head of payload and scientific developments department, «Ghalam» LLP, Astana, Kazakhstan; SCOPUS Author ID: 57350754500; <http://orcid.org/0000-0001-5926-9619>; [b.zhumazhanov@ghalam.kz](mailto:b.zhumazhanov@ghalam.kz)

**Zhetpisbayeva, Ainur** – PhD, Associate Professor, Department of Radio engineering, electronics, and telecommunications, L.N. Gumilyov Eurasian National University, Astana, Kazakhstan; SCOPUS Author ID: 57189702755; <https://orcid.org/0000-0002-4525-5299>; [aigulji@mail.ru](mailto:aigulji@mail.ru)

**Kulakayeva, Aigul** – PhD, Associate Professor, Department of Radio engineering, electronics, and telecommunications, International Information Technology University, Almaty, Kazakhstan; SCOPUS Author ID: 56732962300; <https://orcid.org/0000-0002-0143-085X>; [a.kulakayeva@iitu.edu.kz](mailto:a.kulakayeva@iitu.edu.kz)

**Makhanov, Kanat** – Candidate of Physical and Mathematical Sciences, Senior Lecturer, Department of Radio engineering, electronics, and telecommunications, L.N. Gumilyov Eurasian National University, Astana, Kazakhstan; Scopus Author ID: 57217354220; <https://orcid.org/0000-0002-1263-0734>; [makanov@inbox.ru](mailto:makanov@inbox.ru). +77009667591

**Zhumazhanov, Bexultan** – Master (Eng.), Design-engineer, «Ghalam» LLP, Astana, Kazakhstan, <https://orcid.org/0009-0000-9493-7491>; [zhumazhanov.b@ghalam.kz](mailto:zhumazhanov.b@ghalam.kz)